KINETIC EFFECTS IN THE HIGH-SPEED DEFORMATION OF ALUMINUM

A. K. Divakov, Yu. I. Meshcheryakov, and L. P. Fadienko

UDC 532.533.539.374

Shock-wave characteristics for A-95, A-6, and D-16 aluminum have been used to examine the relationship between the rate-dependent mechanical properties of materials and the kinetics of elementary plastic-strain processes, particularly the dispersion of the particle mass velocity at the compression-wave front.

A pneumatic gun of size 35 mm [1] was used in the shock loading of specimens in the form of disks of diameter 52 mm. The speed of the projectile was varied over the range 20-270 m/sec. The speed was determined by measuring the time interval required to travel a fixed distance. The error of measurement was not more than 1%.

Two methods were used to measure the time profiles of the velocity at the free surface and the stress profiles: a differential laser interferometer [2] with a delay arm of 11.7 nsec and X-cut quartz piezoelectric transducers working in short-circuit mode [3]. The time profiles for the materials are shown in Figs. 1-3, and these have been used in constructing dynamic σ—ε diagrams. The stresses were determined from equations implied by the elasto-plastic model:

$$\sigma = \rho c u \quad \text{for} \quad u < u_{el}\,, \quad \sigma = \rho c_* (u - u_H) + \sigma_H \quad \text{for} \quad u > u_{el}\,,$$

where c is the longitudinal speed of sound, c_* is the speed of the plastic front, and σ_H is the Hugoniot elastic limit. To improve the reliability, the maximum velocity was determined in two ways: by measuring the speed of the projectile and from the form of the interferogram in terms of the number of signal beats on the leading and trailing edges of the compression pulse. Figures 1-3 show that the wave profiles have a plateau corresponding to the maximum surface velocity.

The plastic-wave speed was determined from $c_* = d(t_e + \Delta t_p)$, where d is the target thickness (2-15 mm in the experiments), t_e is the time of transit of the elastic wave through the target, and Δt_p is the time interval between the elastic precursor and the plastic front. In accordance with the analysis of [4], this interval should be reckoned between the midpoints of the elastic and plastic fronts. Figure 4 shows the speed of the plastic front as a function of the speed of the free surface for A-6 and A-95 aluminum (lines 1 and 2 correspondingly).

The dynamic σ—ε diagrams were derived by determining the elastic constants: bulk modulus, Lamé constants, and so on, for which purpose precision ultrasonic measurements were made of the longitudinal and transverse speeds of sound. Table 1 gives the results.

Table 2 gives the shock-wave characteristics, from which one can construct dynamic σ—ε diagrams. For greater clarity, Fig. 5 shows $\sigma_d - \sigma_h$ as a function of free-surface velocity for A-95 and A-6 (lines 1 and 2 correspondingly, where σ_d is the stress corresponding to the dynamic diagram and σ_h is that corresponding to the hydrostatic curve). Figure 5 shows that $\sigma_d - \sigma_h$ increases linearly with the loading rate, and the slope for A-95 is higher than that for A-6. Therefore, both materials show mechanical properties dependent on the strain rate,

TABLE 1

Material	$c_{\parallel}$, m/sec	$c_{\perp}$, m/sec	ρ, g/cm^3
A-95	6427±10	3185±5	2,67
A-6	6444±6	3140±5	2,70
D-16	6396±15	3120±60	2,75

Leningrad. Translated from Zhurnal Prikladnoi Mekhaniki i Tekhnicheskoi Fiziki, No. 1, pp. 123-127, January-February, 1984. Original article submitted December 17, 1982.

0021-8944/84/2501-0111$08.50

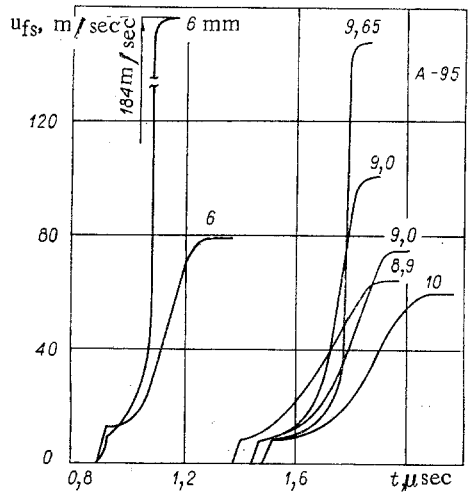

Fig. 1

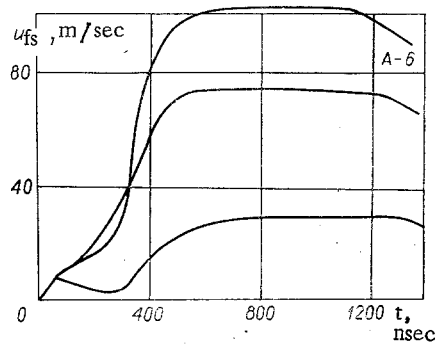

Fig. 2

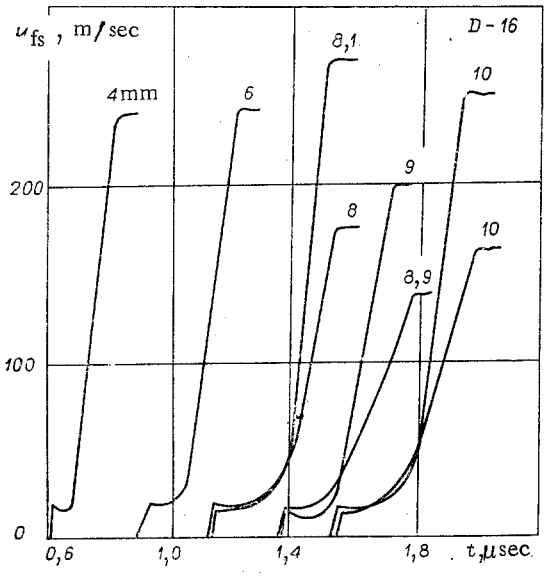

Fig. 3

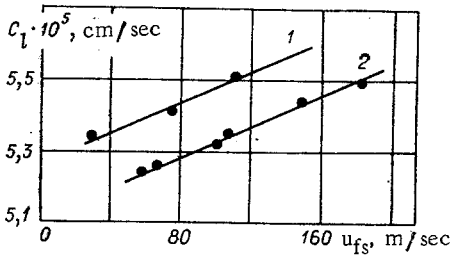

Fig. 4

and A-95 more than A-6. A difference from these materials is that the dynamic diagram for D-16 constructed from the data of Table 2 runs parallel to the hydrostatic compression curve throughout the loading range, as occurs in materials not showing rate-dependent effects.

The most interesting results appears to be that there is a single-valued relationship between the rate dependence of the mechanical properties on the one hand and the elementary plastic-strain processes on the other. The larger the particle speed dispersion in the wave for the material, the less the dependence on the strain rate. This follows from a comparison of the dynamic characteristics with the corresponding interference signals. A specific feature of interferometry in free-surface speed measurement is that one can record the particle velocity distribution. The analysis of [5] shows that the principle used in deriving an interference pattern from a moving surface means that if the surface has a velocity distribution (i.e., dispersion in the mass velocity), then the best amplitude in the interferometric signal decreases. If the distribution is sufficiently wide and comparable with the interferometer constant, the beat amplitudes may become zero.

The interferograms of Fig. 6 were recorded with identical projectile velocities of about 66 m/sec for A-95 and D-16, and they confirm that the rate dependence of the mechanical properties is correlated with the dispersion in the particle velocity. The curves show that there is an interference pattern for the compression pulse for A-95, with a pronounced dependence on the strain rate, the elastic precursor showing 0.75 beat, the plastic front 2 beats, and the trailing edge 2.75 beats, whereas for D-16 there is no beat picture for the plastic front,

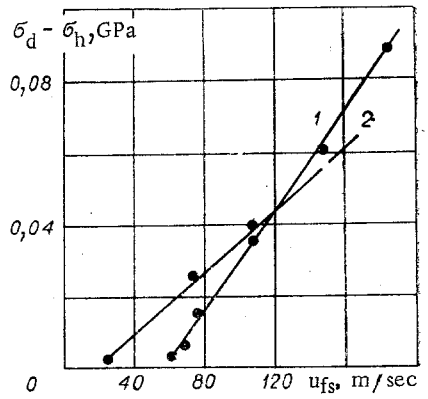

Fig. 5

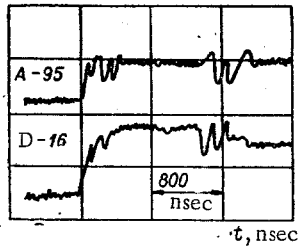

Fig. 6

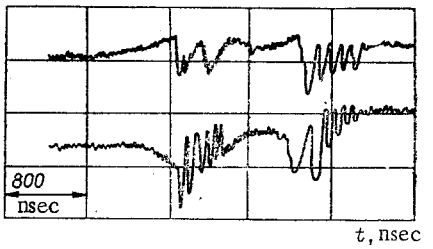

Fig. 7

TABLE 2

Material	Projectile speed, m/sec	Target thickness, mm	Projectile thickness, mm	Plastic front speed, km/sec	Maximum stress, GPa	Deformation $\%\cdot10^{-3}$
D-16	106	8,9	5	5,47	0,805	9,68
	66	8,9	5	5,47	0,502	6,32
	132	8,9	5	5,48	1,005	12,04
	205	8,9	5	5,49	1,564	18,67
	230	9,0	5	5,51	17,32	21,20
	160	10	2	5,52	1,188	14,50
	246	10	2	5,48	1,874	22,44
	267	8,1	2	5,53	1,994	22,50
	174	8,0	2	5,51	1,333	15,76
	241	6,0	2	5,51	1,849	21,80
	240	4,0	2	5,44	1,814	22,00
A-95	66	9,0	5	5,27	0,470	6,27
	60	9,7	5	5,26	0,426	5,70
	106	9,6	5	5,37	0,770	9,90
	102	9,4	5	5,34	0,732	9,50
	80	6,0	5	5,30	0,571	7,54
	147	9,65	2	5,44	1,079	13,76
	184	6,0	2	5,50	1,366	16,70
A-6	74,5	9,35	5	5,42	0,545	6,87
	109	9,4	5	5,50	0,772	9,93
	27	9,4	5	5,34	0,195	2,52

although the elastic precursor and the trailing edge are quite clear cut. There is also no beat on the leading edge in D-16 at other loading rates. Another point is also clear: a marked reduction in the beat amplitude due to the free-surface particle velocity dispersion that occurs only with nonstationary plastic fronts, whereas stationary ones always show a fairly clear-cut interference picture. The compression waves in A-95 and A-6 aluminum become stationary at very small distances from the collision surface (about 1.5 mm) in the loading rate range used, and they correspond to patterns with pronounced beat structure. On the other hand, in D-16 at these loading rates the wave settling terminates at depths of about 10-15 mm, i.e., the compression wave is still not stationary at the time the plastic front is recorded. On the other hand, it is well known [6] that the higher the stress amplitude in the compression wave, the more rapidly it becomes stationary. This explains why the beat pattern for the leading edge becomes more pronounced as the loading rate increases. This is confirmed by the interferograms of Fig. 7, which correspond to identical D-16 targets at different loading rates. The elastic precursor with 3/4 beat is seen on the upper pattern, after which there is a relaxation zone. A plateau of length about 0.8 μm separates the leading edge from the trailing one, in which the velocity of the free surface is constant. The interferograms show that there are no beats on the leading edge, whereas the trailing one corresponds to five beats. Instead of those beats at the leading edge, there is a bell-shaped pulse for the plastic front, whose duration is equal to the length of the leading edge and the vertex corresponds to the middle of it. The lower interferogram was recorded at a higher loading rate, and here both edges have beat patterns.

We are indebted to A. I. Nedbaya for carrying out the ultrasonic measurements in order to determine the elastic constants.

LITERATURE CITED

1. Yu. I. Meshcheryakov, V. A. Morozov, and Yu. V. Suden'kov, "Experimental methods of examining highly nonequilibrium processes in solids on exposure to pulsed electron beams and high-speed collision," in: Physical Mechanics [in Russian], Issue 2, Izd. LGU, Leningrad (1978).
2. L. M. Barker, Behavior of Dense Media under High Dynamic Pressure, Gordon and Breach, New York (1968).
3. R. A. Graham, F. W. Neilson, and W. B. Benedic, "Piezoelectric current from shock loaded quartz: a submicrosecond stress gauge," J. Appl. Phys., 36, No. 5 (1965).
4. L. M. Barker, "α-phase Hugoniot in iron," J. Appl. Phys., 46, No. 6 (1975).
5. J. R. Asay and L. M. Barker, "Interferometric measurements of shock-induced internal particle velocity and spatial variation of particle velocity," J. Appl. Phys., 45, No. 6 (1974).
6. J. N. Johnson and L. M. Barker, "Dislocation dynamics and steady plastic wave profile in 6061-T6 aluminum," J. Appl. Phys., 40, No. 11 (1969).

PORE GROWTH IN SLIP BANDS IN LOCALIZED PLASTIC STRAIN

V. M. Segal

UDC 539.375.5

Pore behavior in a plastically deformed material is of considerable interest in relation to viscous failure [1]. Solutions have been obtained [2, 3] for isolated pores acted on by homogeneous stress and velocity fields applied at infinity; a continuum description has also been given [4, 5] of a plastically dilating material containing a pore ensemble. In all cases it is assumed that the flow in the region of the pores is stable, while the initial spherical or cylindrical shape remains close to equilibrium.

On the other hand, a feature common to all plastic bodies is that the flow is unstable which leads to regions of highly localized strain [6]. Such regions are observed at the microscopic and macroscopic levels as thin shear bands, within which the strain intensity is higher than that in parts outside by several orders of magnitude. The geometrical or material instability [6] determines whether the shear bands occupy fixed positions within the flow regions (lines of velocity discontinuity for the rigid-plastic body) or certain volumes in the deformed material (grain boundaries and other structural imperfections). Also, they can be observed not only directly after the start of plastic flow but also in the final stages preceding failure.

Flow localization and the subsequent strain in slip bands are closely related to pore nucleation and growth. It has been suggested [7] that the localization is due to softening arising from the increase in porosity. An alternative view [6] relates the localization to detailed features of the constructive equations. However, no matter what the reasons, localization produces a considerable reduction in the plasticity because the strain is concentrated in small volumes and a specific mechanism occurs for pore growth in the shear bands. The latter is accompanied by the formation of pore layers, in which viscous cracks grow and the material fails. As the thicknesses of the shear bands hardly alter during this process, it is clear that the pore shape becomes nonequilibrium at the localization stage, while the change in pore size occurs mainly in the shear planes. This conclusion is confirmed by analogous stability-loss phenomena for pores in pure shear in elastic and viscous materials [8]. Neglect of this feature should result in one substantially overestimating the plasticity parameters, as is observed in the analysis of viscous failure in shear bands [9, 10] based on an isotropic pore growth mechanism [5].

Here we present a simple model for pore behavior during plastic-strain localization, which involves pronounced anisotropy in the growth rates in the shear plane and in the normal direction. The results are applied in examining the formation of viscous cracks along velocity-discontinuity lines for a rigid-plastic material in pressure-working of metals.

Minsk. Translated from Zhurnal Prikladnoi Mekhaniki i Tekhnicheskoi Fiziki, No. 1, pp. 127-134, January-February, 1984. Original article submitted November 10, 1982.

0021-8944/84/2501-0114$08.50